

Active-controlled cascaded proton acceleration using a solenoid driven by picosecond laser pulse

Research Article

Cite this article: Shi Z *et al.* (2025) Active-controlled cascaded proton acceleration using a solenoid driven by picosecond laser pulse. *Laser and Particle Beams* **43**, e2, 1–6. <https://doi.org/10.1017/lpb.2025.1>

Received: 29 October 2024
Revised: 25 March 2025
Accepted: 12 April 2025

Keywords:

cascade acceleration; high energy density physics; proton acceleration; proton beam shaping; proton imaging

Corresponding author: Wenpeng Wang;
Email: wangwenpeng@siom.ac.cn
Weimin Zhou; Email: wmzhou@caep.cn
Yuxin Leng; Email: lengyuxin@mail.siom.ac.cn

Zhiyong Shi¹, Wenpeng Wang¹, Xinyu Xie^{1,2}, Jianzhi He^{1,3}, Hao Dong^{1,3}, Xinyue Sun^{1,2}, Hua Huang⁴, Bo Zhang⁴, Lei Yang⁴, Zhigang Deng⁴, Feng Lu⁴, Weimin Zhou⁴, Yuqiu Gu⁴, Yuxin Leng^{1,2,3}, Ruxin Li^{1,2,3} and Zhizhan Xu^{1,2,3}

¹State Key Laboratory of Ultra-intense Laser Science and Technology, Shanghai Institute of Optics and Fine Mechanics, Chinese Academy of Sciences, Shanghai, China; ²University of Chinese Academy of Sciences, Beijing, China; ³School of Physical Science and Technology, Shanghai Tech University, Shanghai, China and ⁴National Key Laboratory of Plasma Physics, Laser Fusion Research Center, China Academy of Engineering Physics (CAEP), Mianyang, China

Abstract

An actively controllable cascaded proton acceleration driven by a separate 0.8 picosecond (ps) laser is demonstrated in proof-of-principle experiments. MeV protons, initially driven by a femtosecond laser, are further accelerated and focused into a dot structure by an electromagnetic pulse (EMP) on the solenoid, which can be tuned into a ring structure by increasing the ps laser energy. An electrodynamics model is carried out to explain the experimental results and show that the dot-structured proton beam is formed when the outer part of the incident proton beam is optimally focused by the EMP force on the solenoid; otherwise, it is overfocused into a ring structure by a larger EMP. Such a separately controlled mechanism allows precise tuning of the proton beam structures for various applications, such as edge-enhanced proton radiography, proton therapy and pre-injection in traditional accelerators.

Introduction

High-quality proton beams produced by laser-driven thin solid foils (Refs 1–6) can be used in various fields such as proton therapy (Refs 7, 8), proton imaging (Ref. 9) and fast ignition of inertial confinement fusion (Ref. 10). Several mechanisms have been proposed for energetic proton generation, such as radiation pressure acceleration (RPA) (Refs 11–14), collisionless shock acceleration (CSA) (Ref. 15), target normal sheath acceleration (TNSA) (Ref. 16), breakout afterburner acceleration (Ref. 17) and other combined mechanisms (Refs 18, 19). To date, TNSA is still considered the most robust acceleration mechanism for obtaining ~100 MeV proton beams (Ref. 20). However, these ion beams typically exhibit broad energy spectra or large beam divergence, limiting their direct application in fields like proton therapy (Refs 7, 8). To address this, a cascaded acceleration mechanism based on the robust TNSA mechanism has been developed (Refs 21–23), where a sheath field generated on a second target tailors the spectra and maximum energy of the incident proton beam from the first acceleration stage (Refs 23, 24).

However, the previous cascaded mechanisms were inefficient because only a small fraction (usually $\ll 10\%$) of the incident proton beam from the first stage is accelerated by the finite static sheath field driven by the small focal spot of the second laser on the second target (Refs 22, 25). Recently, Kar *et al.* proposed a post-processing scheme by using a femtosecond (fs) laser to drive a metallic foil attached to a solenoid to improve the cascaded acceleration efficiency. The main reason is that the electromagnetic pulse (EMP) driven by the laser on the solenoid can synchronise with the incident protons under an optimal space–time condition to further accelerate and collimate the incident proton beam for a longer time and larger distance (Refs 25–31). However, since the solenoid is directly connected to the target's back, it limits the ability to flexibly tune the parameters of the incident protons and the solenoid independently, resulting in the limited tuning for the energy, spectra and divergence of the proton beam. Therefore, separating the solenoid from the target may be an efficient method to potentially introduce more innovations to the present cascaded solenoid acceleration mechanism.

In this article, we present an actively controllable cascaded proton acceleration mechanism driven by a separated picosecond (ps) laser in experiments. It is found that an fs-laser irradiates the target to generate MeV protons in the first stage, which are further tuned by an EMP on an independent solenoid irradiated by another ps laser in the second stage. An electrodynamics

© The Author(s), 2025. Published by Cambridge University Press. This is an Open Access article, distributed under the terms of the Creative Commons Attribution licence (<http://creativecommons.org/licenses/by/4.0>), which permits unrestricted re-use, distribution and reproduction, provided the original article is properly cited.

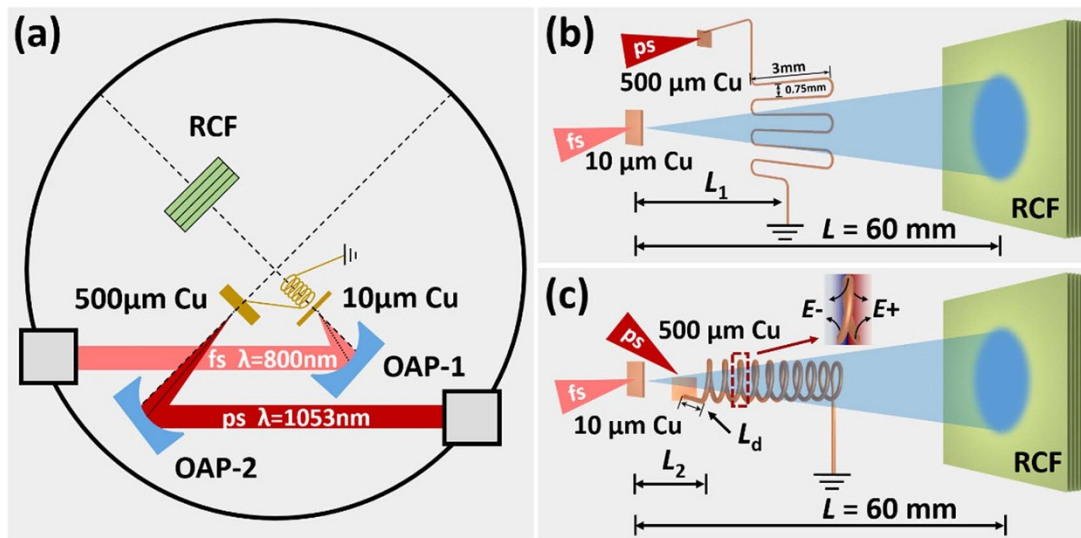


Figure 1. (a) Experimental setup. The fs laser drives a 10 μm copper to generate a proton beam, and the ps laser drives a 500 μm copper to generate an EMP to modulate the proton beam. (b) Proton imaging setup. The diameter of the folded copper wire was 0.1 mm, with a width of ~ 3 mm and a vertical spacing of ~ 0.75 mm between wires. (c) Active-controlled cascaded proton acceleration setup. The solenoid was constructed with 0.1 mm diameter copper wire, with an inner diameter of ~ 0.7 mm, a pitch of ~ 0.3 mm, 10 turns, and an overall length of ~ 3 mm.

model is carried out to explain the experimental results, showing that the proton beam can be shaped into ring and dot forms by appropriately tuning the EMP strength on the solenoid, which is consistent with the experimental results. The proton beam shapes tailored in our ps-laser-driven cascaded solenoid acceleration mechanism offer a convenient and controllable method for creating structured proton beams for special applications. For instance, the ring proton beam can enhance edge-imaging in proton radiography for expanding plasma and capsule implosions in confined fusion, while the collimated proton beam can be used for proton therapy.

Experimental setup

The experiment was conducted at the XingGuang-III laser facility in the Laser Fusion Research Center (see Fig. 1a). An ~ 8 J fs laser with a wavelength of 800 nm and a duration of ~ 50 fs irradiated a 10 μm thick copper target, accelerating a proton beam via the TNSA mechanism in the first stage. In the second stage, a ps laser with ~ 30 J to ~ 120 J energy and ~ 800 fs duration (full width at half maximum (FWHM)) was focused onto a 500 μm thick copper foil. One side of a folded wire was connected to the foil back, and the other side to the ground, generating an EMP towards the ground when the ps laser irradiated the copper foil. The resulting longitudinal and transverse electric fields in the solenoid centre moved forward, continuously accelerating and concentrating the proton beam. The radii of the fs and ps laser focal spots were ~ 10 μm and ~ 20 μm , respectively, with about 30% of laser energy enclosed within the FWHM of the focal spots. This corresponds to intensities of $\sim 6.1 \times 10^{19}$ W/cm² for the fs laser and $\sim 3.6 \times 10^{18}$ W/cm² to $\sim 1.4 \times 10^{19}$ W/cm² for the ps laser.

To investigate the effects of the ps-laser-driven solenoid on cascaded proton tailoring, a proton radiograph for the EMP was conducted in Fig. 1b. An fs laser irradiated a separate 10 μm thick copper foil to generate a proton beam to probe the EMP on the folded wire. The 10 μm copper foil was placed at a distance of $L_1 = 6$ mm from the folded wire plane and $L = 60$ mm from

the radiochromic film (RCF) stack, providing a magnification of $M = 10$ on the RCF stacks. The probing beam was oriented perpendicular to the folded wire plane and could be deflected mainly by the electric field on the wire (Ref. 32). By analysing the redistribution of the proton beam on the RCFs, the EMP strength was calculated to understand its effects on proton beam shapes when the folded wire was replaced with a solenoid.

Then, the cascaded solenoid acceleration was implemented by replacing the folded wire with the solenoid in Fig. 1c. The ps-laser energy was increased to ~ 120 J to drive a stronger EMP on the solenoid. By adjusting L_2 (the distance between the 10 μm Cu foil and the front of the solenoid) and L_d (the length of the 500 μm Cu foil and the solenoid connection line), the simultaneous arrival of the proton beam and EMP at the solenoid can be achieved. The EMP propagating along the solenoid forms a helical electric field, exerting a repulsive force on the proton beam and altering its direction and speed.

Experimental results

Figure 2a shows the proton imaging of the copper wire without EMP, where the copper wire width of 1 mm is obtained on RCF. When a ~ 37 J ps laser is introduced in the second stage, the width of the copper wire increases significantly because the incident proton beam from the first stage is dispersed by the EMP moving along the copper wire, see Fig. 2b and c. By analysing the position of the EMP, its propagating velocity ($\sim 0.95 c$) can be calculated, which is consistent with previous research (Refs 33, 34).

According to the EMP velocity and position, we performed the cascade acceleration experiment (see Fig. 1c). Initially, the solenoid is imaged by a 3.4 MeV proton beam from the first stage driven by the 7.7 J fs laser, while the ps laser does not work in Fig. 2d. It can be found that the solenoid separates the incident proton beam into inner and outer regions and the protons distribute uniformly inside the solenoid. In contrast, the 1.6 MeV proton beam with a ring structure was obtained by a ~ 114 J ps laser irradiating on the solenoid in the second stage in Fig. 2e, where the EMP is generated

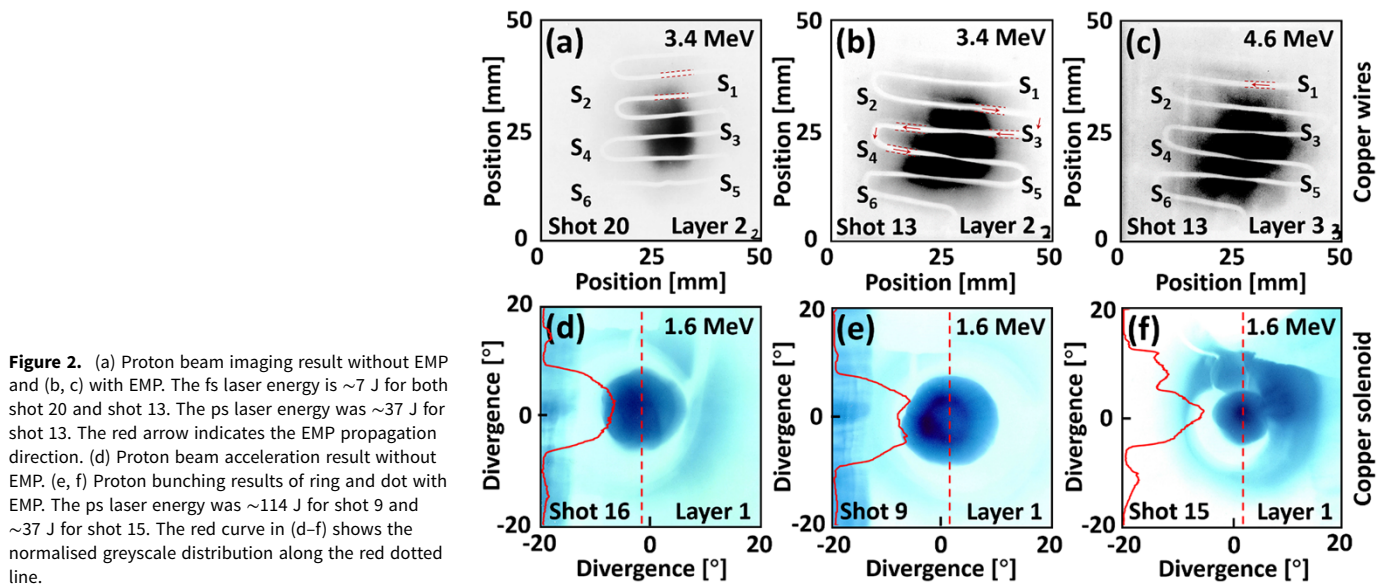


Figure 2. (a) Proton beam imaging result without EMP and (b, c) with EMP. The fs laser energy is ~ 7 J for both shot 20 and shot 13. The ps laser energy was ~ 37 J for shot 13. The red arrow indicates the EMP propagation direction. (d) Proton beam acceleration result without EMP. (e, f) Proton bunching results of ring and dot with EMP. The ps laser energy was ~ 114 J for shot 9 and ~ 37 J for shot 15. The red curve in (d–f) shows the normalised greyscale distribution along the red dotted line.

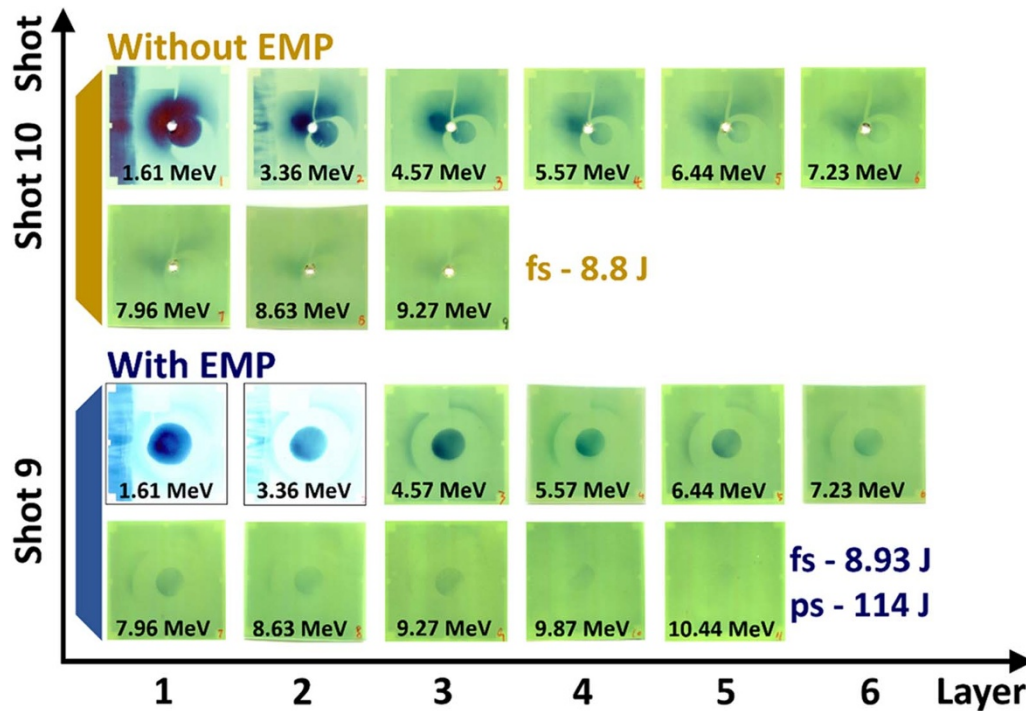


Figure 3. Comparison of the influence of EMP on the proton acceleration.

on the solenoid and manipulates the incident protons inside. It is interesting that the proton structure can transform from ring to dot by reducing the ps laser energy from 114 J down to 37 J (see Fig. 2f). It indicates that proton beam structure can be simply controlled by the EMPs driven by ps lasers with different laser energies or intensities (Refs 26, 29, 30, 35), which will be explained in the following theoretical calculations.

It is important to note that during the preparation of the experiment, we focused on imaging the proton beam on the RCF. We can estimate the maximum cut-off energy of the proton beam by counting the number of RCF pieces. Figure 3 presents a comparison of two proton acceleration results. Shot 9 was conducted with

a ps laser, while shot 10 utilised a separate fs laser. As shown in the comparison, the introduction of the EMP not only enhances the convergence of the proton beam but also leads to an increase in the highest energy order of the proton beam. In future studies, we will explore methods to measure the energy spectrum of the proton beam without compromising the imaging process.

Modelling and analysis

To calculate the intensity and pulse width of the EMP generated by a ps laser, a proton deflection model was developed based on the theory in reference (Ref. 32), as shown in Fig. 4a. The electrostatic

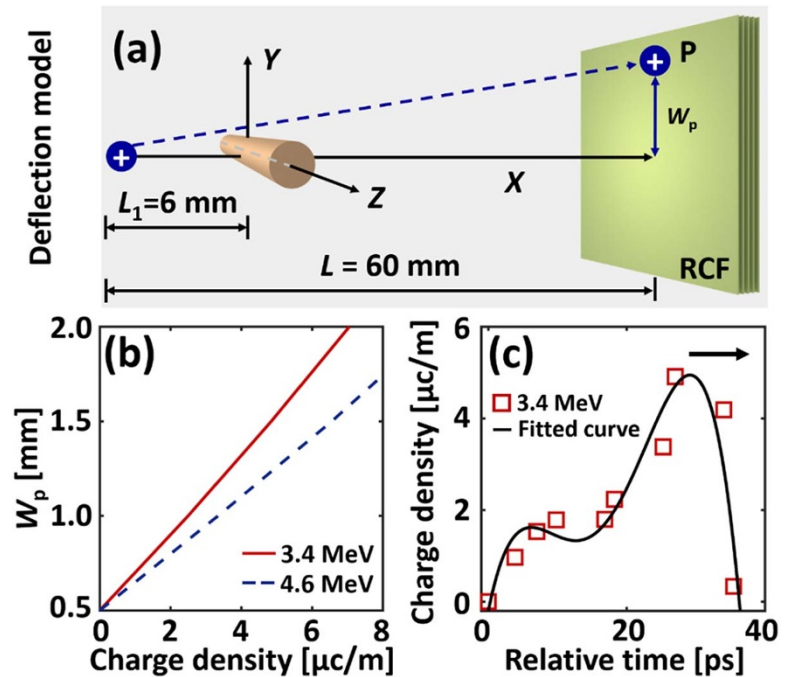


Figure 4. (a) Proton deflection model. (b) Relationship between the charge density and the deflection distance. Here, the solid red line indicates 3.4 MeV, and the blue dotted line indicates 4.6 MeV. (c) Charge density and the relative time calculated from the experimental results. The measured value is the width of the wire at different locations on the RCF. The red squares are the measured values. The solid black line is the fitting curve. The black arrow indicates the direction of EMP propagation.

field \vec{E} in the x - y plane ($z = 0 \mu\text{m}$) is expressed as

$$\vec{E}(0, 0, z) = \int_{-\infty}^{+\infty} \frac{\lambda(z)\vec{r}}{4\pi\epsilon_0 r^3} dz \quad (x^2 + y^2 > R_{\text{Cu}}^2), \quad (1)$$

where ϵ_0 is the permittivity constant of vacuum, \vec{r} is the radius away from the wire centre $(0, 0, z)$. Then, a single proton is incident from the position $(-L_1, 0, 0)$ and is influenced by the electrostatic field from the wire, described by a dynamic equation as

$$\frac{d}{dt} \left(\frac{v}{\sqrt{1-\beta^2}} \right) = \frac{e}{m_i} \vec{E}(0, 0, z), \quad (2)$$

where e is the electron charge, m_i is the ion mass, and $\beta = v/c$ is the dimensionless velocity vector. It is assumed that the protons reach the RCF stacks in the experiment when $x = L - L_1$ is obtained. The deflection distance (w_p) is proportional to the charge density, with lower-energy protons deflecting a greater distance at the same charge density, as shown in Fig. 4b. A ~ 20 ps temporal profile of the charge pulse can be reconstructed in Fig. 4c by calculating w_p at different positions along the solenoid in Fig. 2b and c), which is roughly consistent with previous parameters under similar experimental conditions (Ref. 26). It should be noted that the shape of the EMP pulse excited by the ps laser differs slightly from that excited by the fs laser, and there remains a high charge density at the tail. However, the peak charge density of $\sim 4.9 \mu\text{C}/\text{m}$ is much lower, possibly because a thicker Cu foil ($500 \mu\text{m}$) and lower ps laser energy (~ 37 J) are used in our case.

We establish a simple electrodynamic model to analyse the specific process of proton beam converging into different structures under the action of EMP, as shown in Fig. 5a. In this model, two-point charges, spaced 0.7 mm apart, simulate the two-dimensional

electric field distribution when the EMP moves in the solenoid. The quantity of the point charge Q is $\sim 1.4 \times 10^{-11}$ C, which is calculated by the model in Fig. 4a. The x -direction velocity component of the EMP moving through the solenoid V_{EMP} is $\sim 3.4 \times 10^7$ m/s, which can be calculated by the velocity of the EMP propagating through the wire, the inner diameter of the solenoid and the pitch of the solenoid. Between the two-point charges is a group of evenly distributed protons, and according to the experimental results, the proton divergence is approximately $\sim 14^\circ$. In our case, we simulate 9 protons and do not take into account the repulsion between protons. The protons start at the same position as the two-point charges and move forward in the x -direction with different speeds. Since the clearest results obtained from the experiment correspond to a 1.6 MeV proton beam, we set V_p in the model to $\sim 1.75 \times 10^7$ m/s to match the speed of the 1.6 MeV proton beam. Figure 5b presents the results of the dot proton beam obtained through model simulation, where Q is set to $\sim 1.4 \times 10^{-11}$ C. As seen in Fig. 5b, the edge of the proton beam is influenced by the electric field and converges towards the centre, eventually forming a dot density distribution at 60 mm, similar to the experimental result in Fig. 2f. Furthermore, a ring density distribution is observed in the proton beam in Fig. 5c, where Q is set to 2×10^{-11} C, resembling the experimental results in Fig. 2e. It should be noted that, due to computational limitations, our simulation used only 9 protons to model the distribution trend, which is significantly different from experimental conditions. Furthermore, our simplified electrodynamic model did not account for the repulsive forces between protons or the magnetic field produced by the EMP. The simulation results primarily highlight the impact of EMP intensity on the spatial distribution of proton beams. Both experimental and simulation results show that the spatial distribution of proton beams can be modulated by controlling the EMP intensity. In the follow-up research work, we will further improve the model to make it more realistic to explain the experimental results.

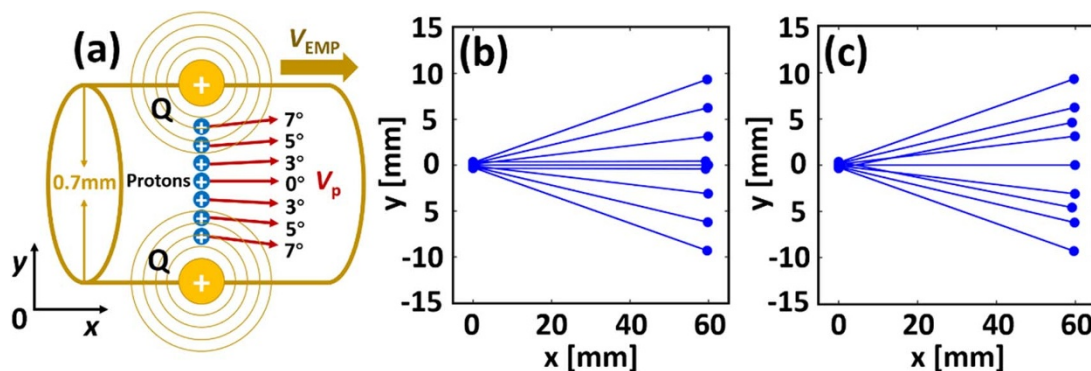


Figure 5. (a) Electrodynamic model. (b, c) The simulation results of the ring and dot proton beams in a 60 mm simulated domain are similar to the experimental results.

Summary

In this article, we propose an active-controllable cascaded proton acceleration mechanism to modulate fs laser proton beams by directing the EMP generated by a ps laser via a solenoid. In the experiment, EMP was initially captured using proton imaging. Subsequent measurements and calculations revealed that the EMP had an FWHM of ~ 20 ps, with a peak intensity of ~ 4.9 $\mu\text{C}/\text{m}$. The solenoid then directed an EMP to effectively shape the proton beam, resulting in the successful generation of both ring and dot configurations of the proton beam. Based on the experimental setup, we established a simple electrostatics model to analyse the experimental results. Our experimental results and simulations have shown that the shape of the proton beam is closely related to the EMP emission. This active-controllable cascaded proton acceleration mechanism can independently adjust the proton beam and EMP, providing a wider adjustment range than the single-beam laser drive method. It offers a solution to produce special-shaped proton beams required in various applications. For example, the ring proton beam has the potential to enhance edge-enhanced proton radiography, such as in expanding plasma studies, while the dot proton beam with lower divergence is of great interest in proton therapy and other fields.

Data availability statement. The data that support the findings of this study are available within the article.

Acknowledgements. This work was supported by the Strategic Priority Research Program of the Chinese Academy of Sciences (Grant No. XDA0380000), Science and Technology Commission of Shanghai Municipality (Grant No. 22DZ1100300), International Partnership Program of Chinese Academy of Sciences (Grant No. 111GJHZ2022029FN), National Natural Science Foundation of China (Grant No. 12388102).

Author contributions. The authors contributed equally to this work.

Conflict of interest. The authors have no conflicts to disclose.

References

- Bai RX, Zhou CT, Huang TW, Jiang K, Ju LB, Li R, Peng H, Yu MY, Qiao B, Ruan SC and He XT (2021) Enhanced proton acceleration using split intense femtosecond laser pulses. *Plasma Physics & Controlled Fusion* **63**(8), 085007. doi:10.1088/1361-6587/abffb9
- Goodman J, King M, Wilson R, Gray RJ and McKenna P (2022) Optimisation of multi-petawatt laser-driven proton acceleration in the relativistic transparency regime. *New Journal of Physics* **24**(5), 053016. doi:10.1088/1367-2630/ac681f
- Isayama S, Chen SH, Liu YL, Chen HW and Kuramitsu Y (2021) Efficient hybrid acceleration scheme for generating 100 MeV protons with tabletop dual-laser pulses. *Physics of Plasmas* **28**(7), 073101, doi:10.1063/5.0049725
- Zimmer M, Scheuren S, Ebert T, Schaumann G, Schmitz B, Hornung J, Bagnoud V, Rodel C and Roth M (2021) Analysis of laser-proton acceleration experiments for development of empirical scaling laws. *Physical Review E* **104**(4–2), 045210. doi:10.1103/PhysRevE.104.045210
- Wang WP, Dong H, Shi ZY, Leng YX, Li RX and Xu ZZ (2022) Collimated particle acceleration by vortex laser-induced self-structured “plasma lens”. *Applied Physics Letters* **121**(21), 214102.
- Yang YC, Zhou CT, Huang TW, He MQ, Wu SZ, Cai TX, Qiao B, Yu MY, Ruan SC and He XT (2020) Manipulating laser-driven proton acceleration with tailored target density profile. *Plasma Physics & Controlled Fusion* **62**(8), 085008. doi:10.1088/1361-6587/ab97f3
- Linz U and Alonso J (2016) Laser-driven ion accelerators for tumor therapy revisited. *Physical Review Accelerators and Beams* **19**(12), 124802, doi:10.1103/PhysRevAccelBeams.19.124802
- Smith AR (2006) Proton therapy. *Physics in Medicine & Biology* **51**(13), R491. doi:10.1088/0031-9155/51/13/R26
- Wang WP, Dong H, Shi ZY, Jiang C, Xu Y, Zhang ZX, Wu FX, Hu JB, Qian JY, Zhu JC, Liang XY, Leng YX, Li RX and Xu ZZ (2023) All-optical edge-enhanced proton imaging driven by an intense vortex laser. *Physics of Plasmas* **30**(3), 033108.
- Naumova N, Schlegel T, Tikhonchuk VT, Labaune C, Sokolov IV and Mourou G (2009) Hole Boring in a DT Pellet and Fast-Ion Ignition with Ultraintense Laser Pulses. *Physical Review Letters* **102**(2), 025002. doi:10.1103/PhysRevLett.102.025002
- Esirkepov T, Borghesi M, Bulanov SV, Mourou G and Tajima T (2004) Highly Efficient Relativistic-Ion Generation in the Laser-Piston Regime. *Physical Review Letters* **92**(17), 175003. doi:10.1103/PhysRevLett.92.175003
- Yan XQ, Lin C, Sheng ZM, Guo ZY, Liu BC, Lu YR, Fang JX and Chen JE (2008) Generating High-Current Monoenergetic Proton Beams by a Circularly Polarized Laser Pulse in the Phase-Stable Acceleration Regime. *Physical Review Letters* **100**(13), 135003. doi:10.1103/PhysRevLett.100.135003
- Macchi A, Veghini S and Pegoraro F (2009) “Light Sail” Acceleration Reexamined. *Physical Review Letters* **103**(8), 085003. doi:10.1103/PhysRevLett.103.085003
- Qiao B, Zepf M, Borghesi M, Dromey B, Geissler M, Karmakar A and Gibbon P (2010) Radiation-Pressure Acceleration of Ion Beams from Nanofoil Targets: The Leaky Light-Sail Regime. *Physical Review Letters* **105**(15), 155002. doi:10.1103/PhysRevLett.105.155002
- Silva LO, Marti M, Davies JR, Fonseca RA, Ren C, Tsung FS and Mori WB (2004) Proton Shock Acceleration in Laser-Plasma Interactions. *Physical Review Letters* **92**(1), 015002. doi:10.1103/PhysRevLett.92.015002
- Wilks SC, Langdon AB, Cowan TE, Roth M, Singh M, Hatchett S, Key MH, Pennington D, MacKinnon A and Snavely RA (2001) Energetic proton generation in ultra-intense laser–solid interactions. *Physics of Plasmas* **8**(2), 542. doi:10.1063/1.1333697

17. Yin L, Albright BJ, Hegelich BM and Fernández JC (2006) GeV laser ion acceleration from ultrathin targets: The laser break-out afterburner. *Laser and Particle Beams* 24(2), 291.
18. Higginson A, Gray RJ, King M, Dance RJ, Williamson SDR, Butler NMH, Wilson R, Capdessus R, Armstrong C, Green JS, Hawkes SJ, Martin P, Wei WQ, Mirfayzi SR, Yuan XH, Kar S, Borghesi M, Clarke RJ, Neely D and McKenna P (2018) Near-100 MeV protons via a laser-driven transparency-enhanced hybrid acceleration scheme. *Nature Communications* 9(1), 724. doi:10.1038/s41467-018-03063-9
19. Henig A, Kiefer D, Markey K, Gautier DC, Flippo KA, Letzring S, Johnson RP, Shimada T, Yin L, Albright BJ, Bowers KJ, Fernandez JC, Rykovanov SG, Wu HC, Zepf M, Jung D, VKh Liechtenstein JS, Habs D and Hegelich BM (2009) Enhanced Laser-Driven Ion Acceleration in the Relativistic Transparency Regime. *Physical Review Letters* 103(4), 045002. doi:10.1103/PhysRevLett.103.045002
20. Hornung J, Zobus Y, Boller P, Brabetz C, Eisenbarth U, Kühl T, Zs Major JBO, Zepf M, Zielbauer B and Bagnoud V (2020) Enhancement of the laser-driven proton source at PHELIX. *High Power Laser Science and Engineering* 8 1–8.
21. Pfoth SM, Jäckel O, Polz J, Steinke S, Schlenvoigt HP, Heymann J, Robinson APL and Kaluza MC (2010) A cascaded laser acceleration scheme for the generation of spectrally controlled proton beams. *New Journal of Physics* 12(10), 103009. doi:10.1088/1367-2630/12/10/103009
22. Wang WP, Shen BF, Zhang H, Lu XM, Li JF, Zhai SH, Li SS, Wang XL, Xu RJ, Wang C, Leng YX, Liang XY, Li RX and Xu ZZ (2018) Multi-stage proton acceleration controlled by double beam image technique. *Physics of Plasmas* 25(6), 063116.
23. Wang WP, Shen BF, Zhang H, Lu XM, Li JF, Zhai SH, Li SS, Wang XL, Xu RJ, Wang C, Leng YX, Liang XY, Li RX and Xu ZZ (2019) Spectrum tailoring of low charge-to-mass ion beam by the triple-stage acceleration mechanism. *Physics of Plasmas* 26(4), 043102.
24. Wang HC, Weng SM, Liu M, Chen M, He MQ, Zhao Q, Murakami M and Sheng ZM (2018) Ion beam bunching via phase rotation in cascading laser-driven ion acceleration. *Physics of Plasmas* 25(8), 083116.
25. Sun XY, Wang WP, Dong H, He JZ, Shi ZY, Leng YX, Li RX and Xu ZZ (2023) Cascaded solenoid acceleration of vortex laser-driven collimated proton beam. *Plasma Physics & Controlled Fusion* 65(9), 095008. doi:10.1088/1361-6587/ace8ba
26. Kar S, Ahmed H, Prasad R, Cerchez M, Brauckmann S, Aurand B, Cantono G, Hadjisolomou P, Lewis CL, Macchi A, Nersisyan G, Robinson AP, Schroer AM, Swantusch M, Zepf M, Willi O and Borghesi M (2016) Guided post-acceleration of laser-driven ions by a miniature modular structure. *Nature Communications* 7, 10792. doi:10.1038/ncomms10792
27. Jiang K, Zhou CT, Huang TW, Ju LB, Wu CN, Li L, Zhang H, Wu SZ, Cai TX, Qiao B, Yu MY and Ruan SC (2019) Divergence and direction control of laser-driven energetic proton beam using a disk-solenoid target. *Plasma Physics & Controlled Fusion* 61(7), 075004. doi:10.1088/1361-6587/ab1d00
28. Ferguson S, Martin P, Ahmed H, Aktan E, Alanazi M, Cerchez M, Doria D, Green JS, Greenwood B, Odlozilik B, Willi O, Borghesi M and Kar S (2023) Dual stage approach to laser-driven helical coil proton acceleration. *New Journal of Physics* 25(1), 013006. doi:10.1088/1367-2630/acaf99
29. Ahmed H, Hadjisolomou P, Naughton K, Alejo A, Brauckmann S, Cantono G, Ferguson S, Cerchez M, Doria D, Green J, Gwynne D, Hodge T, Kumar D, Macchi A, Prasad R, Willi O, Borghesi M and Kar S (2021) High energy implementation of coil-target scheme for guided re-acceleration of laser-driven protons. *Scientific Reports* 11(1), 699. doi:10.1038/s41598-020-77997-w
30. Bardon M, Moreau JG, Romagnani L, Rousseaux C, Ferri M, Lefèvre F, Lantuéjoul I, Etchessahar B, Bazzoli S, Farcage D, Maskrot H, Serres F, Chevrot M, Loyez E, Vuillot E, Cayzac W, Vauzour B, Boutoux G, Sary G, Compant La Fontaine A, Gremillet L, Poyé A, Humières ED and Tikhonchuk VT (2020) Physics of chromatic focusing, post-acceleration and bunching of laser-driven proton beams in helical coil targets. *Plasma Physics & Controlled Fusion* 62(12), 125019. doi:10.1088/1361-6587/abbe35
31. Liu Z, Mei Z, Kong D, Pan Z, Shirui X, Gao Y, Shou Y, Wang P, Cao Z, Liang Y, Peng Z, Zhao J, Chen S, Song T, Chen X, Xu T, Yan X and Ma W (2023) Synchronous post-acceleration of laser-driven protons in helical coil targets by controlling the current dispersion. *High Power Laser Science and Engineering* 11 1–12
32. Ehret M, Bailly-Grandvaux M, Ph Korneev JIA, Brabetz C, Morace A, Bradford P, d'Humières E, Schaumann G, Bagnoud V, Malko S, Matveevskii K, Roth M, Volpe L, Woolsey NC and Santos JJ (2023) Guided electromagnetic discharge pulses driven by short intense laser pulses: Characterization and modeling. *Physics of Plasmas* 30(1), 013105.
33. Quinn K, Wilson PA, Cecchetti CA, Ramakrishna B, Romagnani L, Sarri G, Lancia L, Fuchs J, Pipahl A, Toncian T, Willi O, Clarke RJ, Neely D, Notley M, Gallegos P, Carroll DC, Quinn MN, Yuan XH, McKenna P, Liseykina TV, Macchi A and Borghesi M (2009) Laser-Driven Ultrafast Field Propagation on Solid Surfaces. *Physical Review Letters* 102(19), 194801. doi:10.1103/PhysRevLett.102.194801
34. Ahmed H, Kar S, Cantono G, Nersisyan G, Brauckmann S, Doria D, Gwynne D, Macchi A, Naughton K, Willi O, Lewis CLS and Borghesi M (2016) Investigations of ultrafast charge dynamics in laser-irradiated targets by a self probing technique employing laser driven protons. *Nuclear Instruments and Methods in Physics Research Section A: Accelerators, Spectrometers, Detectors and Associated Equipment* 829, 172. doi:10.1016/j.nima.2016.04.078.
35. Aktan E, Ahmed H, Aurand B, Cerchez M, Poyé A, Hadjisolomou P, Borghesi M, Kar S, Willi O and Prasad R (2019) Parametric study of a high amplitude electromagnetic pulse driven by an intense laser. *Physics of Plasmas* 26(7), 070701, doi:10.1063/1.5094871.